Electronic Supplementary Material (ESI) for Soft Matter.

Supplementary Information

for

Structure and Thermodynamics of Mixed Polymeric Micelles with Crystalline Cores: Tuning Properties via Co-Assembly

Nico König,[1,2] Lutz Willner,[2,*] and Reidar Lund[1,†]

[1] *Department of Chemistry, University of Oslo, Postboks 1033 Blindern, 0315 Oslo, Norway*
[2] *Jülich Centre for Neutron Science JCNS and Institute for Complex Systems ICS, Forschungszentrum Jülich GmbH, 52425 Jülich, Germany*

FITS OF C_{12}- AND C_{14}-PEO SAXS DATA

The scattering data of C_{12}- and C_{14}-PEO are shown separately here because they require special treatment since the critical micellar concentration (CMC) of these polymers is close to the experimental concentrations. Thus for these samples concentration-dependent measurements were performed at only one temperature, $T = 25\,°C$. In the scattering data in figure S1 it is eminent that micellar scattering only emerges above a certain concentration threshold. Thus, the model was amended by unimer scattering in the form of an additional Beaucage form factor, see reference [1] for details. The fit parameters are given in table S1. Unfortunately, the CMC and the aggragtion number are highly correlated fit parameters. Therefore, even though the fits shown in figure S1 are the best fits, there is a large uncertainty in N_{agg} and acceptable fits can still be obtained with aggregation numbers which are more in line with a $N_{agg} \propto n^2$ scaling for small n. See the main manuscript for details.

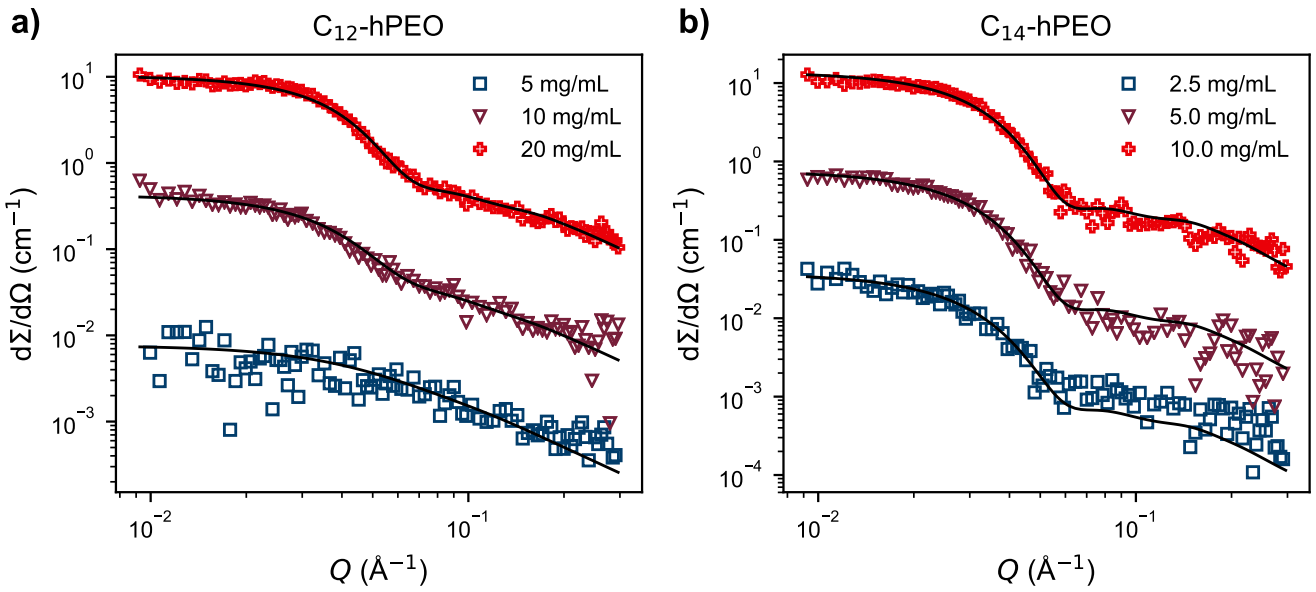

FIG. S1: Scattering data of a) C_{12}- and b) C_{14}-hPEO at various concentrations around the CAC at 25 °C. Solid lines represent a simultaneous fit of all concentrations according to the model presented in reference [1] and fit parameters are given in table S1.

TABLE S1: SAXS model parameters of C_{12}- and C_{14}-hPEO shown in figure S1

	C_{12}-hPEO	C_{14}-hPEO
N_{agg} [a]	8^{+10}_{-3}	13^{+12}_{-2}
R_m [a] (Å)	70 ± 10	79 ± 6
d_{Cn} [b] (g/mL)	0.75	0.76
R_c [c] (Å)	$8.9^{+4.2}_{-1.3}$	$11.0^{+2.7}_{-0.9}$
d_{PEO} (g/mL)	1.20	1.20
$R_{g,chain}$ [a] (Å)	36 ± 1	39 ± 1
CMC [a] (mg/mL)	6.2 ± 1.5	0.4 ± 0.2
ρ_c (10^{10} cm^{-2})	7.30	7.40
ρ_s (10^{11} cm^{-2})	1.11	1.11
ρ_0 (10^{10} cm^{-2})	9.43	9.43

[a] free fit parameter [b] taken from reference [2]
[c] derived from N_{agg} and d_{Cn}

SCALING ANALYSIS OF MICELLES WITH CRYSTALLINE CORES

As mentioned in the main manuscript, there has been a theoretical treatment of micelles with crystalline cores[3] already. However, this work dealt with long solvophobic blocks that repeatedly fold to form the micellar core. Also, there is a treatment of micelles with rod-like solvophobic blocks[4] which does not consider the enthalpic gain upon crystallization. The polymeric model system under investigation in the present manuscript, C_n-PEO, unites both characteristics. On the one hand, the alkyl blocks crystallize partially within the micellar core. On the other hand, the blocks are relatively short, with a contour length of $L = (15\text{-}27) \times \cos\frac{109.5^\circ}{2} \times 1.54\,\text{Å} = 13.3\text{-}24.0\,\text{Å}$. Comparing the Kuhn length of poly(ethylene), $l_K = 14\,\text{Å}$,[5] it is clear that the alkyl blocks can be considered rod-like. Thus it is hard to conceive a packing order for the partially crystallizing, rod-like alkyl blocks to form a spherical core. Indeed, we have experimental evidence that the micellar cores are aspherical and the effect of crystallisation on the core geometry will be topic of a forthcoming paper. A straightforward way to form the core is by aligning the alkyl block longitudinally into a cylindrical shape, with the PEO corona chains attached to the basal planes. With sufficiently long PEO blocks coiling around the core, the overall shape of the micelle would still appear spherical, in agreement with the reported scattering data. This has also been suggested by Halperin and Vilgis.[3, 4] In line with their argumentation, the total free energy of the micelle comprises three terms:

$$F_{\text{mic}} = F_{\text{core}} + F_{\text{corona}} + F_{\text{interface}}, \tag{1}$$

the contributions from the core, the corona and the interface in between. Traditionally, F_{core} considers stretching penalties of the core block but here it will reflect the enthalpic gain of crystallization. F_{corona}, however, reflects the conventional stretching entropy of the corona blocks which are grafted to the core surface and $F_{\text{interface}}$ contains the surface energy between the solvophobic core and the solvent-swollen corona.

Each alkyl block consists of n CH_2 units with diameter a so that the contour length is $L = na$. We assume the core has a cylindrical shape with radius R_c and thickness L and comprises N_{agg} molecules. Consequently, the area of one of the two basal interfaces is $S_b = N_{\text{agg}}a^2 = \pi R_c^2$ and thus $R_c = \left(N_{\text{agg}}a^2/\pi\right)^{1/2}$. Then the lateral interface is $S_l = 2\pi R_c L = 2na^2\left(\pi N_{\text{agg}}\right)^{1/2}$. This results in the interfacial energy per molecule

$$F_{\text{interface}} = \frac{2\gamma_b S_b}{N_{\text{agg}}} + \frac{\gamma_l S_l}{N_{\text{agg}}} = 2\gamma_b a^2 + 2\gamma_l n a^2 \left(\frac{\pi}{N_{\text{agg}}}\right)^{1/2}, \tag{2}$$

with the interfacial tensions γ_b and γ_l of the basal and lateral interfaces, respectively.

For the coronal free energy, we follow the arguments of Halperin[6] for star-like micelles which will not be recapitulated here. In the leading order, the free energy per molecule resulting from stretching of the corona blocks scales as

$$F_{\text{corona}} \propto N_{\text{agg}}^{1/2} k_B T. \tag{3}$$

We assume each CH_2 unit immersed in the crystalline core gains a hypothetical enthalpy amount H_c so that every alkyl block fully buried in the core gains nH_c. For molecules located at the lateral interface of the cylindrical core, we assume an enthalpy gain of $nH_c/2$ from crystalline interaction. We can calculate the number of molecules at the lateral interface as

$$N_l = \frac{2\pi R_c}{a} = 2\left(\pi N_{\text{agg}}\right)^{1/2}. \tag{4}$$

Therefore, the core contribution to the free energy per molecule is

$$F_{\text{core}} = -\frac{N_l n H_c}{2N_{\text{agg}}} - \frac{(N_{\text{agg}} - N_l) n H_c}{N_{\text{agg}}} = nH_c\left[\left(\frac{\pi}{N_{\text{agg}}}\right)^{1/2} - 1\right]. \tag{5}$$

As we are only interested in the scaling behavior with respect to the aggregation number, we will now drop all irrelevant prefactors as well as terms independent of N_{agg}:

$$F_{\text{mic}} \propto \frac{\gamma_l n a^2}{N_{\text{agg}}^{1/2}} + N_{\text{agg}}^{1/2} k_B T + \frac{nH_c}{N_{\text{agg}}^{1/2}}. \tag{6}$$

Minimization with respect to N_{agg} yields

$$N_{\mathrm{agg}} \propto \frac{\gamma_l n a^2 + n H_c}{k_B T}. \tag{7}$$

Thus our considerations lead to a linear dependency of N_{agg} on n, similar to the apporaches of Halperin and Vilgis[3, 4]. Unfortunately, they fail to explain the $N_{\mathrm{agg}} \propto n^3$ behavior found experimentally which must originate from circumstances not reflected in our calculations.

INDIVIDUAL INSPECTION OF THE MELTING POINTS OF C_{28}- AND C_{22}-PEO

As described in the main manuscript, the melting point of the alkyl block within the micellar core is affected by two phenomena simultaneously: on the one hand, the melting point is influenced by the other component's presence and, on the other hand, it is suppressed because of the self-confinement in the core. We tried to separate these two effects under the assumption of simple additivity. Due to the presence of the other respective component, the melting point is altered to

$$T_m^{0\dagger} = T_m^0 + x\Delta T_m, \tag{8}$$

where T_m^0 is the bulk melting point of C_{22} or C_{28}, respectively, x the fraction of the other respective component and ΔT_m the melting point difference between both components. This altered melting point is furthermore reduced due to the Gibbs-Thomson effect as explained in the main manuscript,

$$T_m = T_m^{0\dagger} - \frac{\alpha\gamma V_{\mathrm{Cn}} T_m^0}{\Delta H_m}. \tag{9}$$

Here, V_{Cn} is the molar volume of C_{22} or C_{28}, respectively, and ΔH_m is the melting enthalpy of the mixture. Figure S2 shows the data for C_{22} and C_{28} individually. Only data at 15 and 65 °C are shown because at those temperatures all mixtures are either frozen or molten, respectively. It is not obvious, though, if $T_m^{0\dagger}$ or T_m^0 should serve as reference point in the numerator of eq. (9). Furthermore, the nature of ΔT_m is not straightforward. For figure S2, the bulk melting point difference $|\Delta T_m| = |T^0_{m,C28} - T^0_{m,C22}| = 17.4\,\mathrm{K}$ has been chosen. But the micellar melting point difference $|\Delta T_m| = |T_{m,C28} - T_{m,C22}| = 27.5\,\mathrm{K}$ is similarly valid. The problem is that ΔT_m is simultaneously affected by the confinement. Thus, no consistent conclusion on the individual effects on C_{22} and C_{28} can be drawn.

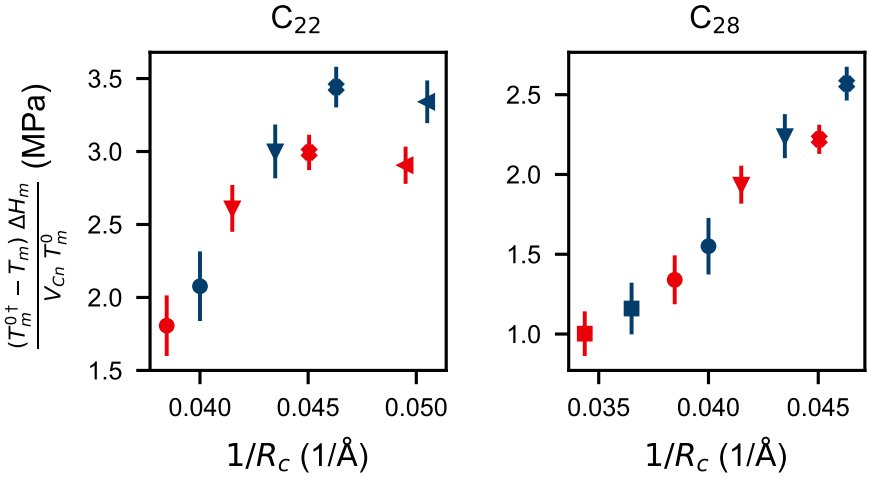

FIG. S2: Individual inspection of the Gibbs-Thomson effect on C_{22} and C_{28} at 15 °C (blue) and 65 °C (red). See text for further explanation.

SUPPLEMENTARY FIGURES

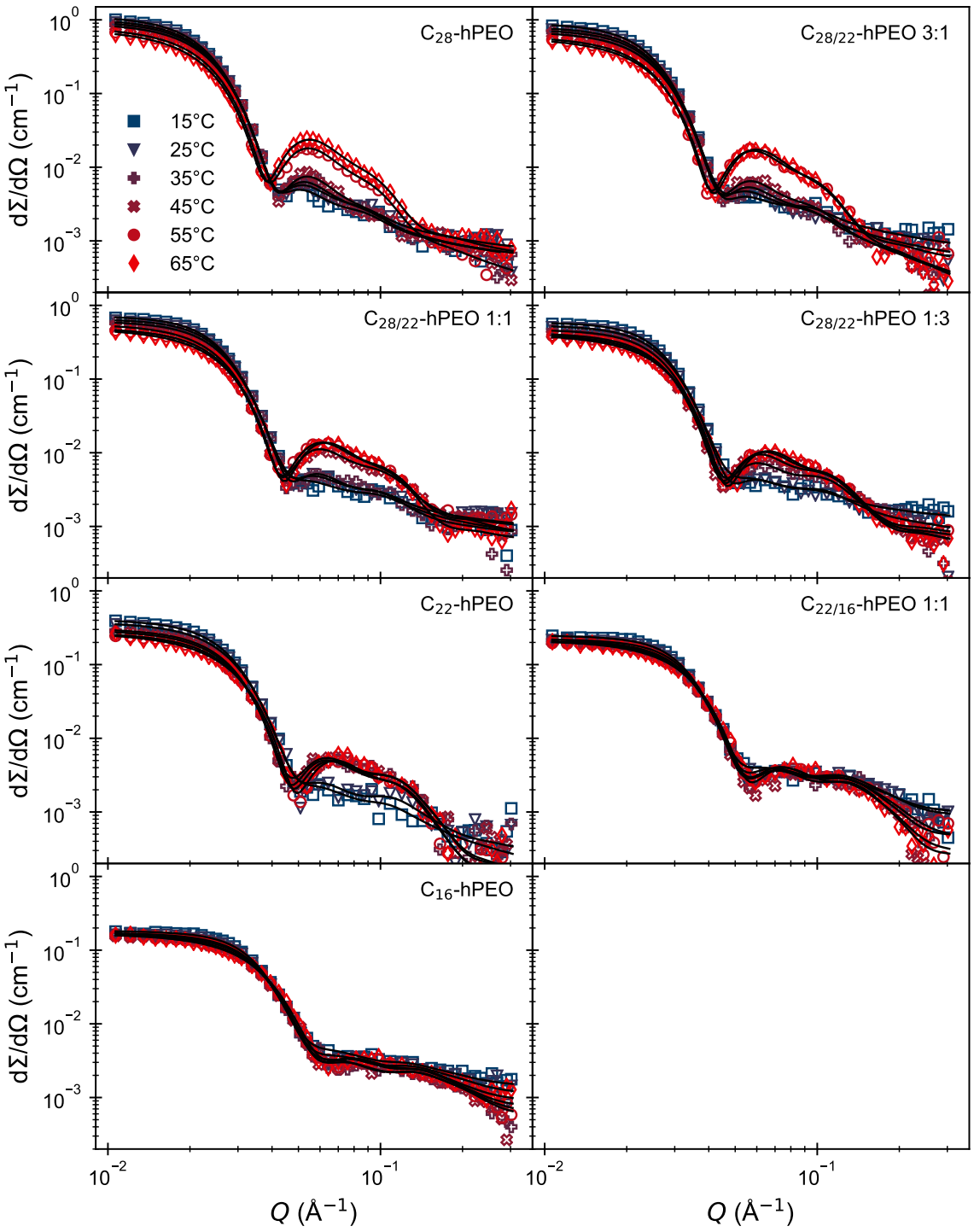

FIG. S3: SAXS data of C_n-hPEO

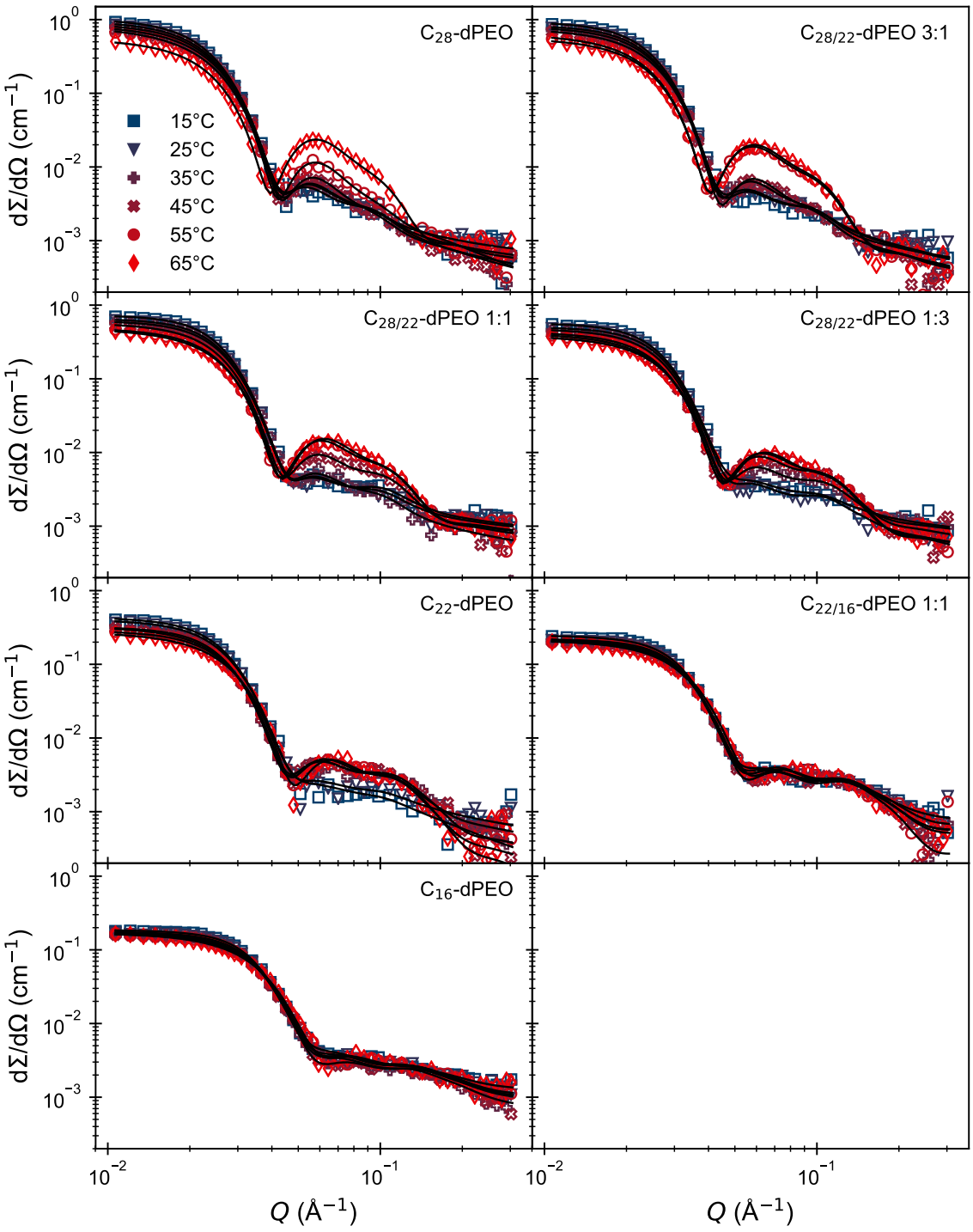

FIG. S4: SAXS data of C_n-dPEO

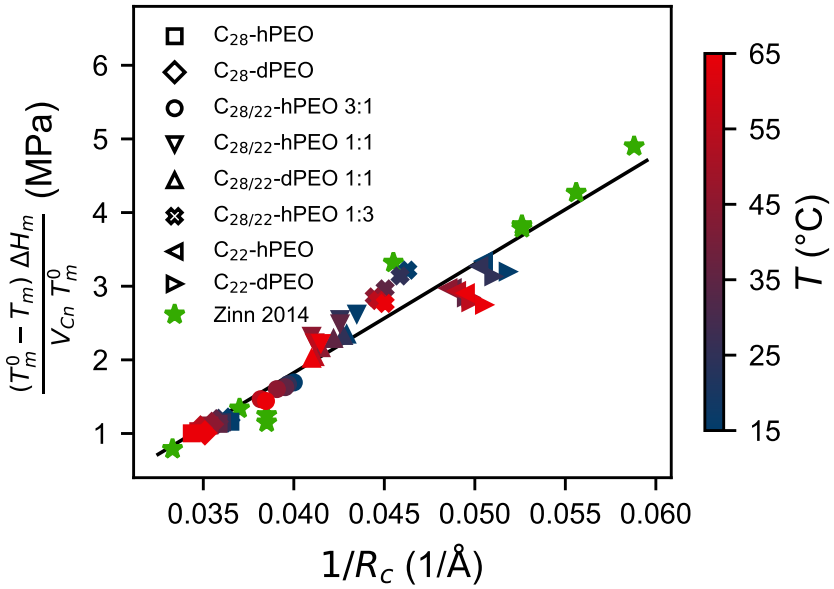

FIG. S5: Reproduction of figure 4 in the main manuscript, containing data from all temperatures: Melting point depression of the alkyl blocks as a result of self-confinement in the micellar core as a function of the inverse core radius. Previously reported data[7] have been added for comparison. The black line is a fit to all data points shown and yields $\gamma = 7.4\,\mathrm{mN/m}$, similar to the value reported in the main manuscript.

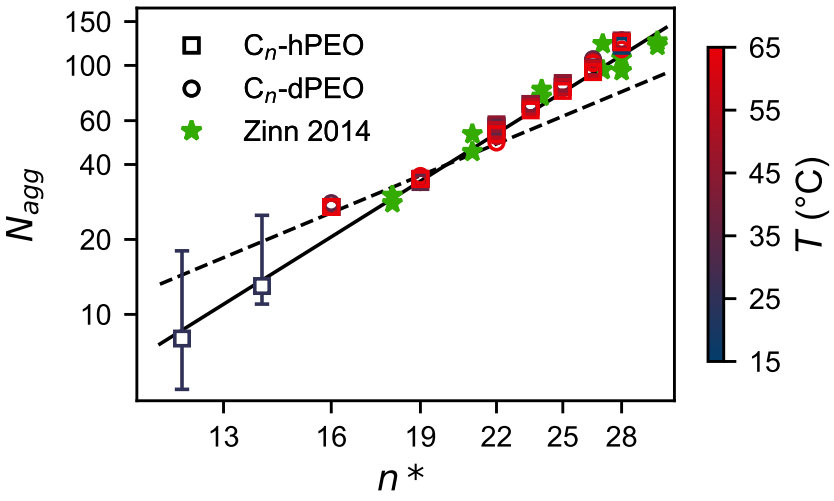

FIG. S6: Aggregation number as a function of the mean alkyl block length, obtained from model fits of SAXS data measured between 15 and 65 °C. Obviously, as the points obtained at different temperatures T overlap, N_{agg} does not depend on T. Previously reported results[8] obtained from the same n-alkyl-PEO system were added for comparison. The dashed line corresponds to $N_{\mathrm{agg}} \propto n^2$, the solid line to $N_{\mathrm{agg}} \propto n^3$.

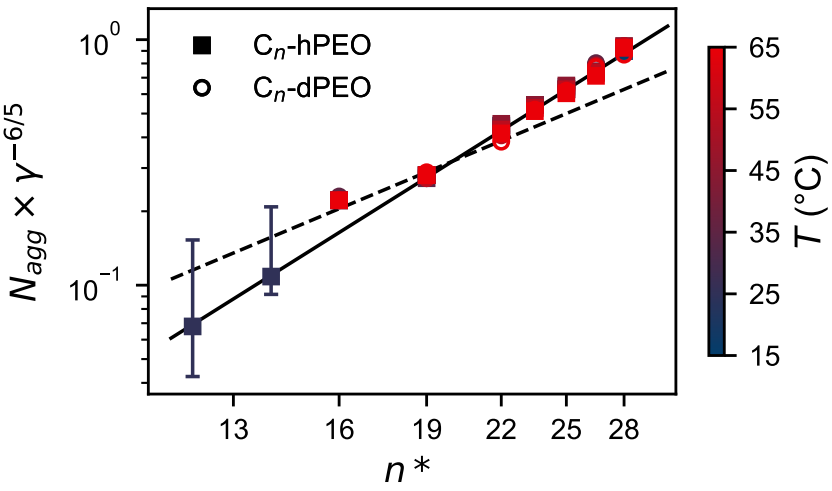

FIG. S7: Aggregation number scaled with the interfacial tension as a function of the mean alkyl block length, obtained from model fits of SAXS data measured between 15 and 65 °C. The dashed line corresponds to $N_{\mathrm{agg}} \propto n^2$, the solid line to $N_{\mathrm{agg}} \propto n^3$.

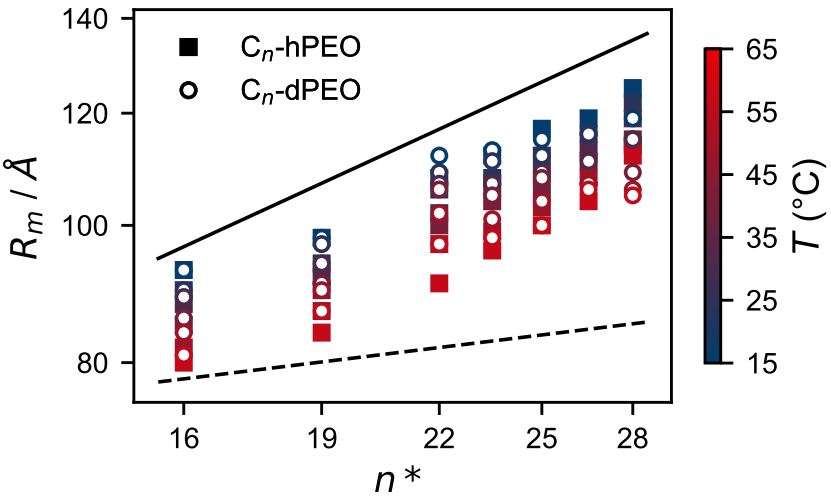

FIG. S8: Micellar radius as a function of the mean alkyl block length, obtained from model fits of SAXS data measured between 15 and 65 °C. The dashed line corresponds to $R_m \propto n^{4/25}$, the solid line to $R_m \propto n^{3/5}$.

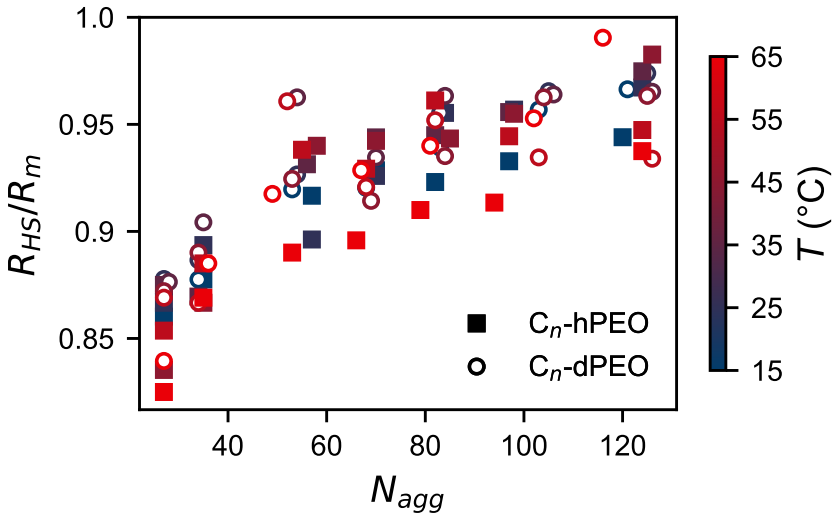

FIG. S9: The hard-sphere interaction radius divided by the micellar radius as a function of the aggregation number. With increasing N_{agg} the corona becomes denser and hence more repellent.

SUPPLEMENTARY TABLES

TABLE S2: SAXS model parameters of C_{28}-hPEO

T (°C)	15	25	35	45	55	65
$N_{\mathrm{agg}}{}^a$	120	124	124	126	124	124
$R_{\mathrm{m}}{}^a$ (Å)	125	122	119	115	114	112
$R_{\mathrm{HS}}{}^a$ (Å)	118	118	116	113	108	105
$d_{\mathrm{Cn}}{}^a$ (g/mL)	0.91	0.90	0.89	0.87	0.81	0.79
R_c (Å)	27.4	27.8	27.9	28.3	28.8	29.1
d_{PEO} (g/mL)	1.21	1.20	1.19	1.17	1.16	1.15
ρ_c ($10^{10}\,\mathrm{cm}^{-2}$)	8.84	8.77	8.62	8.45	7.86	7.65
ρ_s ($10^{11}\,\mathrm{cm}^{-2}$)	1.12	1.11	1.10	1.09	1.08	1.07
ρ_0 ($10^{10}\,\mathrm{cm}^{-2}$)	9.42	9.41	9.38	9.35	9.30	9.26

[a] free fit parameter

TABLE S3: SAXS model parameters of C_{28}-dPEO

T (°C)	15	25	35	45	55	65
$N_{\mathrm{agg}}{}^a$	121	125	126	125	126	116
$R_{\mathrm{m}}{}^a$ (Å)	119	115	115	109	106	105
$R_{\mathrm{HS}}{}^a$ (Å)	115	112	111	105	99	104
$d_{\mathrm{Cn}}{}^a$ (g/mL)	0.91	0.90	0.90	0.87	0.83	0.78
R_c (Å)	27.5	27.9	28.0	28.2	28.7	28.5
d_{PEO} (g/mL)	1.32	1.30	1.29	1.28	1.27	1.25
ρ_c ($10^{10}\,\mathrm{cm}^{-2}$)	8.89	8.77	8.72	8.46	8.10	7.58
ρ_s ($10^{11}\,\mathrm{cm}^{-2}$)	1.12	1.11	1.10	1.09	1.08	1.07
ρ_0 ($10^{10}\,\mathrm{cm}^{-2}$)	9.42	9.41	9.38	9.35	9.30	9.26

[a] free fit parameter

TABLE S4: SAXS model parameters of $C_{28/22}$-hPEO 3:1

T (°C)	15	25	35	45	55	65
$N_{\mathrm{agg}}{}^a$	97	98	97	98	97	94
$R_{\mathrm{m}}{}^a$ (Å)	119	116	113	111	108	104
$R_{\mathrm{HS}}{}^a$ (Å)	111	111	108	106	102	95
$d_{\mathrm{Cn}}{}^a$ (g/mL)	0.92	0.91	0.89	0.87	0.80	0.78
R_c (Å)	25.0	25.2	25.3	25.6	26.2	26.0
d_{PEO} (g/mL)	1.21	1.20	1.19	1.17	1.16	1.15
ρ_c ($10^{10}\,\mathrm{cm}^{-2}$)	8.94	8.82	8.61	8.47	7.74	7.61
ρ_s ($10^{11}\,\mathrm{cm}^{-2}$)	1.12	1.11	1.10	1.09	1.08	1.07
ρ_0 ($10^{10}\,\mathrm{cm}^{-2}$)	9.42	9.41	9.38	9.35	9.30	9.26

[a] free fit parameter

TABLE S5: SAXS model parameters of $C_{28/22}$-dPEO 3:1

T (°C)	15	25	35	45	55	65
$N_{agg}{}^a$	103	105	106	104	103	102
$R_m{}^a$ (Å)	116	116	111	107	107	106
$R_{HS}{}^a$ (Å)	111	112	107	103	100	101
$d_{Cn}{}^a$ (g/mL)	0.91	0.91	0.88	0.86	0.79	0.79
R_c (Å)	25.5	25.7	26.1	26.2	26.8	26.8
d_{PEO} (g/mL)	1.32	1.30	1.29	1.28	1.27	1.25
ρ_c (10^{10} cm^{-2})	8.84	8.84	8.55	8.36	7.71	7.63
ρ_s (10^{11} cm^{-2})	1.12	1.11	1.10	1.09	1.08	1.07
ρ_0 (10^{10} cm^{-2})	9.42	9.41	9.38	9.35	9.30	9.26

[a] free fit parameter

TABLE S6: SAXS model parameters of $C_{28/22}$-hPEO 1:1

T (°C)	15	25	35	45	55	65
$N_{agg}{}^a$	82	84	82	85	82	79
$R_m{}^a$ (Å)	117	112	109	106	103	100
$R_{HS}{}^a$ (Å)	108	107	103	100	99	91
$d_{Cn}{}^a$ (g/mL)	0.92	0.90	0.88	0.82	0.80	0.79
R_c (Å)	23.0	23.5	23.5	24.4	24.3	24.1
d_{PEO} (g/mL)	1.21	1.20	1.19	1.17	1.16	1.15
ρ_c (10^{10} cm^{-2})	9.03	8.77	8.57	8.00	7.76	7.65
ρ_s (10^{11} cm^{-2})	1.12	1.11	1.10	1.09	1.08	1.07
ρ_0 (10^{10} cm^{-2})	9.42	9.41	9.38	9.35	9.30	9.26

[a] free fit parameter

TABLE S7: SAXS model parameters of $C_{28/22}$-dPEO 1:1

T (°C)	15	25	35	45	55	65
$N_{agg}{}^a$	83	83	84	84	82	81
$R_m{}^a$ (Å)	115	112	109	108	104	100
$R_{HS}{}^a$ (Å)	108	107	105	101	99	94
$d_{Cn}{}^a$ (g/mL)	0.91	0.90	0.89	0.84	0.79	0.78
R_c (Å)	23.3	23.4	23.7	24.1	24.3	24.4
d_{PEO} (g/mL)	1.32	1.30	1.29	1.28	1.27	1.25
ρ_c (10^{10} cm^{-2})	8.84	8.78	8.61	8.14	7.69	7.61
ρ_s (10^{11} cm^{-2})	1.12	1.11	1.10	1.09	1.08	1.07
ρ_0 (10^{10} cm^{-2})	9.42	9.41	9.38	9.35	9.30	9.26

[a] free fit parameter

TABLE S8: SAXS model parameters of $C_{28/22}$-hPEO 1:3

T (°C)	15	25	35	45	55	65
$N_{agg}{}^a$	70	70	70	70	68	66
$R_m{}^a$ (Å)	112	108	107	104	88	96
$R_{HS}{}^a$ (Å)	104	100	101	98	92	86
$d_{Cn}{}^a$ (g/mL)	0.92	0.89	0.84	0.81	0.80	0.79
R_c (Å)	21.6	21.8	22.2	22.5	22.4	22.2
d_{PEO} (g/mL)	1.21	1.20	1.19	1.17	1.16	1.15
ρ_c (10^{10} cm^{-2})	8.91	8.69	8.21	7.90	7.76	7.66
ρ_s (10^{11} cm^{-2})	1.12	1.11	1.10	1.09	1.08	1.07
ρ_0 (10^{10} cm^{-2})	9.42	9.41	9.38	9.35	9.30	9.26

[a] free fit parameter

TABLE S9: SAXS model parameters of $C_{28/22}$-dPEO 1:3

T (°C)	15	25	35	45	55	65
$N_{agg}{}^a$	68	68	70	69	68	67
$R_m{}^a$ (Å)	113	111	107	105	101	98
$R_{HS}{}^a$ (Å)	104	103	100	96	93	91
$d_{Cn}{}^a$ (g/mL)	0.91	0.90	0.85	0.81	0.80	0.79
R_c (Å)	21.4	21.5	22.1	22.3	22.4	22.3
d_{PEO} (g/mL)	1.32	1.30	1.29	1.28	1.27	1.25
ρ_c (10^{10} cm^{-2})	8.88	8.77	8.27	7.91	7.76	7.70
ρ_s (10^{11} cm^{-2})	1.12	1.11	1.10	1.09	1.08	1.07
ρ_0 (10^{10} cm^{-2})	9.42	9.41	9.38	9.35	9.30	9.26

[a] free fit parameter

TABLE S10: SAXS model parameters of C_{22}-hPEO

T (°C)	15	25	35	45	55	65
$N_{agg}{}^a$	57	57	56	58	55	53
$R_m{}^a$ (Å)	108	106	102	100	97	91
$R_{HS}{}^a$ (Å)	99	95	95	94	91	81
$d_{Cn}{}^a$ (g/mL)	0.91	0.89	0.81	0.81	0.80	0.79
R_c (Å)	19.8	19.9	20.5	20.6	20.4	20.2
d_{PEO} (g/mL)	1.21	1.20	1.19	1.17	1.16	1.15
ρ_c (10^{10} cm^{-2})	8.84	8.64	7.87	7.87	7.77	7.67
ρ_s (10^{11} cm^{-2})	1.12	1.11	1.10	1.09	1.08	1.07
ρ_0 (10^{10} cm^{-2})	9.42	9.41	9.38	9.35	9.30	9.26

[a] free fit parameter

TABLE S11: SAXS model parameters of C_{22}-dPEO

T (°C)	15	25	35	45	55	65
$N_{agg}{}^a$	53	54	54	53	52	49
$R_m{}^a$ (Å)	112	109	107	106	102	97
$R_{HS}{}^a$ (Å)	103	101	103	87	98	89
$d_{Cn}{}^a$ (g/mL)	0.91	0.89	0.81	0.81	0.79	0.78
R_c (Å)	19.3	19.6	20.2	20.1	20.1	19.8
d_{PEO} (g/mL)	1.32	1.30	1.29	1.28	1.27	1.25
ρ_c (10^{10} cm^{-2})	8.88	8.77	8.27	7.91	7.76	7.70
ρ_s (10^{11} cm^{-2})	1.12	1.11	1.10	1.09	1.08	1.07
ρ_0 (10^{10} cm^{-2})	9.42	9.41	9.38	9.35	9.30	9.26

[a] free fit parameter

TABLE S12: SAXS model parameters of $C_{22/16}$-hPEO

T (°C)	15	25	35	45	55	65
$N_{agg}{}^a$	35	35	34	35	35	35
$R_m{}^a$ (Å)	98	94	92	90	87	84
$R_{HS}{}^a$ (Å)	86	84	80	78	77	73
$d_{Cn}{}^a$ (g/mL)	0.85	0.84	0.83	0.82	0.81	0.80
R_c (Å)	16.3	16.4	16.4	16.6	16.7	16.7
d_{PEO} (g/mL)	1.21	1.20	1.19	1.17	1.16	1.15
ρ_c (10^{10} cm^{-2})	8.30	8.12	8.03	7.96	7.83	7.73
ρ_s (10^{11} cm^{-2})	1.12	1.11	1.10	1.09	1.08	1.07
ρ_0 (10^{10} cm^{-2})	9.42	9.41	9.38	9.35	9.30	9.26

[a] free fit parameter

TABLE S13: SAXS model parameters of $C_{22/16}$-dPEO

T (°C)	15	25	35	45	55	65
$N_{agg}{}^a$	34	34	35	34	34	36
$R_m{}^a$ (Å)	98	97	94	91	90	87
$R_{HS}{}^a$ (Å)	86	86	85	81	78	77
$d_{Cn}{}^a$ (g/mL)	0.85	0.83	0.82	0.81	0.81	0.81
R_c (Å)	16.2	16.3	16.5	16.5	16.5	16.7
d_{PEO} (g/mL)	1.32	1.30	1.29	1.28	1.27	1.25
ρ_c (10^{10} cm^{-2})	8.21	8.10	8.00	7.88	7.84	7.91
ρ_s (10^{11} cm^{-2})	1.12	1.11	1.10	1.09	1.08	1.07
ρ_0 (10^{10} cm^{-2})	9.42	9.41	9.38	9.35	9.30	9.26

[a] free fit parameter

TABLE S14: SAXS model parameters of C_{16}-hPEO

T (°C)	15	25	35	45	55	65
$N_{agg}{}^a$	27	27	27	27	27	27
$R_m{}^a$ (Å)	93	90	88	85	82	80
$R_{HS}{}^a$ (Å)	80	78	77	71	70	66
$d_{Cn}{}^a$ (g/mL)	0.85	0.84	0.83	0.82	0.80	0.80
R_c (Å)	14.1	14.2	14.2	14.3	14.4	14.4
d_{PEO} (g/mL)	1.21	1.20	1.19	1.17	1.16	1.15
ρ_c (10^{10} cm^{-2})	8.25	8.14	8.07	7.99	7.79	7.80
ρ_s (10^{11} cm^{-2})	1.12	1.11	1.10	1.09	1.08	1.07
ρ_0 (10^{10} cm^{-2})	9.42	9.41	9.38	9.35	9.30	9.26

[a] free fit parameter

TABLE S15: SAXS model parameters of C_{16}-dPEO

T (°C)	15	25	35	45	55	65
$N_{agg}{}^a$	27	27	28	27	27	27
$R_m{}^a$ (Å)	93	90	89	86	84	81
$R_{HS}{}^a$ (Å)	81	79	78	75	73	68
$d_{Cn}{}^a$ (g/mL)	0.84	0.83	0.83	0.82	0.81	0.81
R_c (Å)	14.1	14.3	14.4	14.4	14.5	14.4
d_{PEO} (g/mL)	1.32	1.30	1.29	1.28	1.27	1.25
ρ_c (10^{10} cm^{-2})	8.18	8.06	8.08	7.99	7.88	7.85
ρ_s (10^{11} cm^{-2})	1.12	1.11	1.10	1.09	1.08	1.07
ρ_0 (10^{10} cm^{-2})	9.42	9.41	9.38	9.35	9.30	9.26

[a] free fit parameter

REFERENCES

* l.willner@fz-juelich.de
† reidar.lund@kjemi.uio.no

[1] V. A. Bjørnestad, *Liposomes as a model system for the study of surface active peptides*, Master thesis, Department of Chemistry - University of Oslo (2018).
[2] J. R. Rumble (ed.), *CRC Handbook of Chemistry and Physics, 100th Edition (Internet Version 2019)*, edited by J. R. Rumble (CRC Press/Taylor & Francis, Boca Raton, FL, 2019).
[3] T. Vilgis and A. Halperin, Macromolecules **24**, 2090 (1991).
[4] A. Halperin, Macromolecules **23**, 2724 (1990).
[5] M. Rubinstein and R. Colby, *Polymer Physics* (Oxford University Press, 2003).
[6] A. Halperin, Macromolecules **20**, 2943 (1987).
[7] T. Zinn, L. Willner, and R. Lund, Physical Review Letters **113**, 238305 (2014).
[8] T. Zinn, L. Willner, R. Lund, V. Pipich, M. S. Appavou, and D. Richter, Soft Matter **10**, 5212 (2014).